

Reactive intermediates in aqueous ozone decomposition: A mechanistic approach*

István Fábán[‡]

Department of Inorganic and Analytical Chemistry, University of Debrecen,
P.O.B. 21, Debrecen 10, H-4010, Hungary

Abstract: This paper provides a detailed account of recent developments in the mechanistic interpretation of aqueous ozone decomposition. Experimental complications with collecting reliable kinetic information for this system are illustrated via a few examples. Classical and comprehensive data treatment methods are compared, and an advanced kinetic model is presented on the basis of simultaneous evaluation of about 60 kinetic traces recorded at 260, 430, and 600 nm. These are the wavelengths of the absorbance maxima of O₃, O₃⁻, and CO₃⁻, respectively. The model is used to explore specific features of the initiation sequence, the role of reactive intermediates, and the carbonate ion inhibition. It is also demonstrated how a complex kinetic model can be validated by studying the system under specific experimental conditions.

Keywords: ozone; aqueous ozone; reaction mechanism; aqueous ozone decomposition; kinetic models.

INTRODUCTION

Ozone has become a well-known chemical species in recent years owing to its escalating disappearance from the stratosphere. Besides the infamous ozone hole, enhanced formation of ozone from the exhaust systems of motor vehicles in urban areas also generated considerable interest in gas-phase ozone chemistry. Detailed interpretation of the chemical role of ozone in the atmosphere earned the Nobel prize for Crutzen, Molina, and Sherwood in 1995 [1]. In contrast, aqueous phase chemistry of ozone is less publicized and remained mainly the realm of targeted investigations related to practical applications of ozone. Although some of the results obtained for the gas-phase chemical properties of ozone bear relevance to its behavior in condensed phase, there are significant differences between the gaseous and aqueous phase reactions of ozone.

In the aqueous phase, ozone finds widespread applications in disinfection, whitening, water treatment, and oxidation technologies [2–7]. These applications are based on the extreme oxidizing power of ozone, which can react either directly or indirectly with the substrates. Direct oxidation reactions are specific and involve direct attack of O₃ on double bonds. In indirect reactions, the reactive species is the OH radical formed from ozone. The hydroxyl radical is a nondiscriminating oxidant—that is, it is able to oxidize almost any substrate and these reactions lead to complete mineralization of organic compounds if ozone is applied in sufficient excess [4]. In recent years, considerable efforts have been devoted to enhance the oxidation power of ozone by developing advanced oxidation processes (AOPs). In

*Paper based on a presentation at the 29th International Conference on Solution Chemistry, Portorož, Slovenia, 20–25 August 2005. Other presentations are published in this issue, pp. 1559–1617.

[‡]E-mail: ifabian@delfin.unideb.hu

these systems, the formation of the OH radical is typically boosted by the addition of H₂O₂ and/or TiO₂ as well as by irradiation with UV light.

The oxidation reactions of ozone are always coupled with its decomposition. The relative rates of ozone decomposition and the actual oxidation reactions determine the transient concentrations of the reactive intermediates and, as a consequence, the efficiency of the overall oxidation process in terms of ozone consumption. It follows that understanding the intimate details of ozone decomposition is crucial with respect to efficient control of AOPs and other practical applications as well as maintaining an optimal ozone budget in such technologies. The implications of the results are also useful in the assessment of the environmental impact of ozone.

The purpose of this report is to demonstrate the complexity of the decomposition reaction and provide insight into the origin of the main controversies in related literature results. Experimental and computation aspects of developing appropriate kinetic models are covered in detail. It will be shown that advanced kinetic evaluation techniques yield an improved set of reaction steps and make it possible to eliminate some of the uncertainties related to the overall process. The improved model is suitable for the interpretation of the catalytic effect of H₂O₂ and carbonate ion inhibition. This account is intended to be an up-to-date survey of the topic, and most of the data presented here are based on earlier results from our and other laboratories. Details of the experimental protocol are reported in our earlier publications [8,9].

EARLIER KINETIC MODELS FOR AQUEOUS OZONE DECOMPOSITION

The kinetics and mechanism of aqueous phase decomposition of ozone have been studied at different levels for decades. In general, there is an agreement that the decomposition reaction is a complicated radical-type chain reaction [10], although a recent study challenges this view to some extent under acidic conditions [11]. On the basis of available literature data, two fairly detailed kinetic models emerged for the interpretation of the results under neutral–alkaline conditions by the second half of the 1980s [12–16]. While these models include a few common propagation steps, they are essentially different with respect to the initiation steps, the number and significance of the individual chain carriers, and the dominant reaction steps. The models lead to different conclusions regarding basic features of ozone decomposition.

The Tomiyasu, Fukutomi, and Gordon (TFG) model postulates the following initiation sequence



and implies that the main chain carrier is the O₃⁻ radical [16]. The model developed by Staehelin, Bühler, and Hoigné (SBH) originally included different initiation reactions and assumed that HO₃ and HO₄ radicals play an important role in the decomposition [13–15]. In recent studies, the SBH model was somewhat modified by adopting that initiation occurs via eqs. 1 and 2, but other features of the model were not changed. [17]. Our early model calculations serve as clear evidence that neither the TFG nor the SBH models provide sufficient interpretation of the experimental observations in their original forms [18]. It was concluded that additional studies would be required to explore various aspects of the reaction in order to develop a more reliable kinetic model. Most importantly, obvious discrepancies arising from experimental complications and oversimplified evaluation methods needed to be clarified.

EXPERIMENTAL ASPECTS

Aqueous ozone is notorious for its instability, which in turn leads to reproducibility problems in kinetic experiments. At this point, it should be emphasized that there are limited options for monitoring the

overall reaction, and conclusions regarding the reliability of the experiments are solely based on comparisons of the variation of the absorbance as a function of time under similar conditions. Ozone exhibits a characteristic absorbance band at $\lambda_{\max} = 260$ nm, which can be used for monitoring ozone decay in mildly alkaline solution. When the pH is increased, a relatively sharp minimum develops on the kinetic traces, and the contribution from another absorbing species becomes obvious (Fig. 1). These traces can be interpreted as the combination of ozone decay and the formation of O_2^- , which also has measurable absorbance in this wavelength region [16]. At relatively high pH (>12.0), the O_3^- radical is formed in sufficient concentrations and its formation and decay can be studied at its characteristic absorbance band, $\lambda_{\max} = 430$ nm (Fig. 2) [19]. In carefully designed and executed experiments, the CO_3^- radical can also be detected at 600 nm when carbonate ion is added to the reaction mixture [20]. However, in this case, the absorbance change is very small, requiring meticulous assessment of the raw data. It should be noted that reactive intermediates can accumulate at detectable concentration levels only when the ozone decay is relatively fast, thus requiring the use of fast kinetic techniques such as the stopped-flow method.

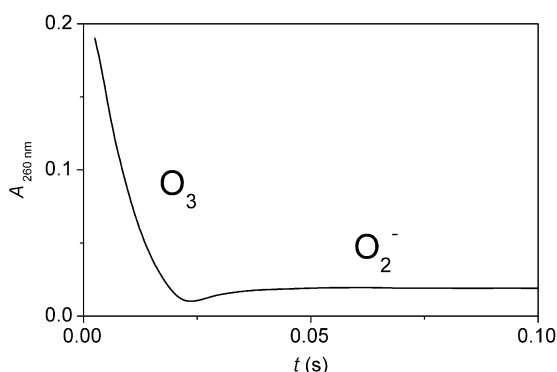


Fig. 1 Typical kinetic trace at 260 nm. $[\text{O}_3]_0 = 7.1 \times 10^{-5}$ M, pH = 13.2, $T = 25$ °C, $I = 0.5$ M NaClO_4 .

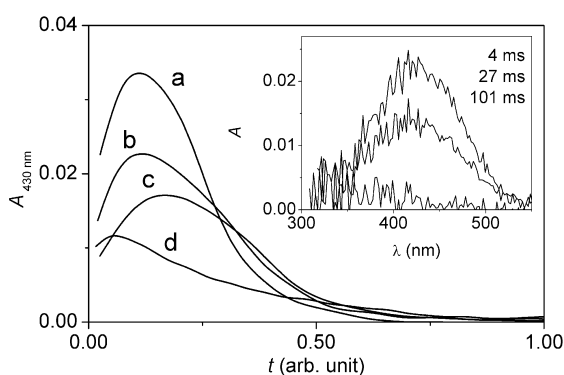


Fig. 2 Typical kinetic traces at 430 nm. $[\text{O}_3]_0 = 7.0 \times 10^{-5}$ M, pH = 13.2, unit time: 0.100 s (a); $[\text{O}_3]_0 = 8.3 \times 10^{-5}$ M, pH = 13.0, unit time: 0.125 s (b); $[\text{O}_3]_0 = 4.5 \times 10^{-5}$ M, pH = 12.8, unit time: 0.100 s (c); $[\text{O}_3]_0 = 9.9 \times 10^{-5}$ M, pH = 12.2, unit time: 0.250 s (d). Inset: time-dependent rapid scan spectra showing the decay of the O_3^- radical. $[\text{O}_3]_0 = 8.3 \times 10^{-5}$ M, pH = 13.2. $T = 25$ °C, $I = 0.5$ M NaClO_4 .

Experimental protocols need to address the high volatility of ozone and the presence of trace amounts of impurities, which may act as promoters or inhibitors of ozone decomposition. Apart from

this, other artefacts may also corrupt the experimental data. Two examples for such problems are described below.

One of the key issues is photochemical decomposition of ozone by the light source of the instruments during photometric kinetic experiments [8]. The absorbance decay after 1000 s continuous irradiation as well as the half-lifetime of ozone is shown as the function of the voltage of the photomultiplier of an APL DX-17 MV stopped-flow instrument in Fig. 3. In this equipment, a Xe lamp is used as a light source and a monochromatic beam irradiates the reaction mixture in single wavelength mode. There is an inverse correlation between the light intensity and the voltage of the photomultiplier tube, that is, the higher the voltage the less light passes the sample. As shown, even monochromatic light at 260 nm has a profound effect on the stability of ozone. In order to avoid complications from this effect, the light intensity of the instrument needs to be minimized such that the absorbance measurements are still reproducible within the usually accepted limits, ± 0.001 AU.

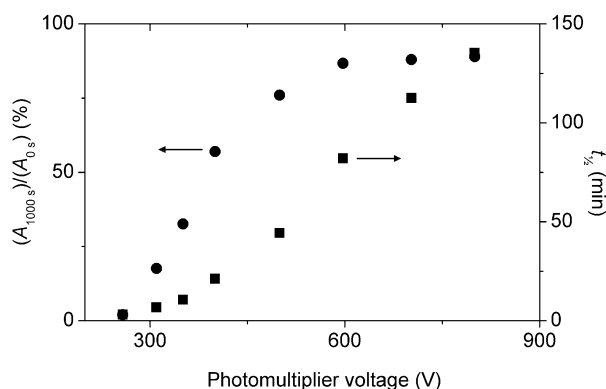
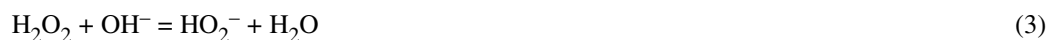


Fig. 3 The effect of light intensity of the stopped-slow instrument on ozone stability. The higher the “photomultiplier voltage” the less light passes the sample. Left axis: absorbance decay compared to the initial absorbance after 1000 s. Right axis: the life-time ozone.

The way ozone stock solutions are prepared also alters the kinetic features of the decomposition [9]. Ozone solutions are prepared by sparging O_3/O_2 gas mixture into slightly acidic aqueous solution. It was shown that increasing the duration of bubbling reduced the lifetime of ozone in subsequent kinetic experiments and also affected the shapes of the kinetic traces (Fig. 4). This effect was interpreted in terms of slow acidic decomposition of ozone into H_2O_2 [21] which accumulates during the preparation of the stock solution. Hydrogen peroxide itself does not react with ozone, but its deprotonated form is a very efficient catalyst of the decomposition. When ozone solution is made alkaline in a kinetic experiment, HO_2^- is rapidly formed via reaction 3 and triggers the fast catalytic path (eq. 2).



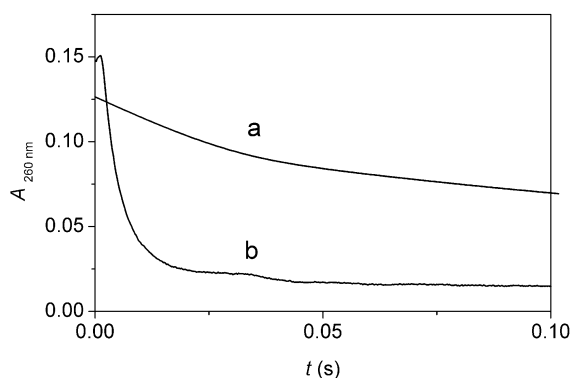


Fig. 4 The effect of ozone generation time on the kinetic traces. Generation times: 7 min (a); 45 min (b). $T = 25\text{ }^{\circ}\text{C}$, $I = 0.5\text{ M NaClO}_4$.

Recent results are in full support of these considerations [22]. As shown in Fig. 5, the amount of H_2O_2 in ozone stock solutions increases by increasing the generation time. In these experiments, the stock solutions were purged with nitrogen in order to remove O_3 , and $[\text{H}_2\text{O}_2]$ was determined by oxidizing Fe(II) and measuring the concentration of Fe(III) spectrophotometrically at 304 nm. The detection limit of the method is $5 \times 10^{-7}\text{ M}$ [22].

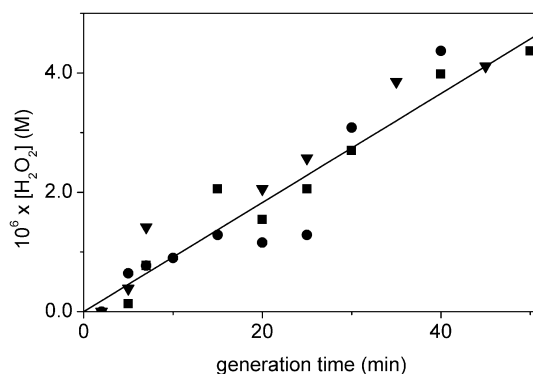


Fig. 5 The accumulation of H_2O_2 in three different ozone stock solutions as a function of ozone generation time.

Detailed studies confirmed that the catalytic route cannot be neglected above $[\text{H}_2\text{O}_2]_0 = 2.0 \times 10^{-6}\text{ M}$. Hydrogen peroxide enhances the formation of the O_2^- radical and affects substantially the kinetic profiles of O_3^- . Accordingly, the concentration of the ozonide ion radical increases and reaches its maximum value at shorter reaction times by increasing $[\text{H}_2\text{O}_2]_0$ (Fig. 6).

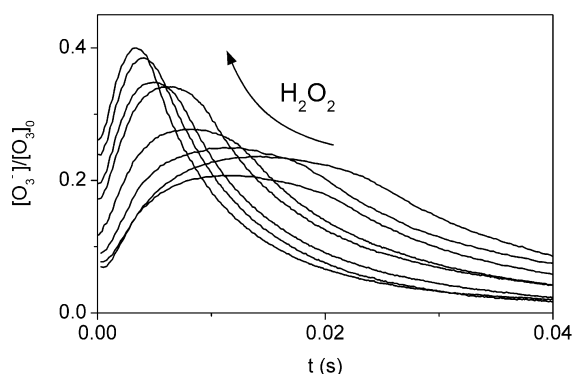


Fig. 6 The effect of hydrogen peroxide concentration on the formation and decay of the O_3^- radical. Conditions in the order of increasing maximum concentration of O_3^- : $[\text{O}_3^-]_0 = 8.27 \times 10^{-5} \text{ M}$, $[\text{H}_2\text{O}_2]_0 = 2 \times 10^{-6} \text{ M}$; $[\text{O}_3^-]_0 = 8.55 \times 10^{-5} \text{ M}$, $[\text{H}_2\text{O}_2]_0 = 5.0 \times 10^{-6} \text{ M}$; $[\text{O}_3^-]_0 = 7.14 \times 10^{-5} \text{ M}$, $[\text{H}_2\text{O}_2]_0 = 8.0 \times 10^{-6} \text{ M}$; $[\text{O}_3^-]_0 = 9.47 \times 10^{-5} \text{ M}$, $[\text{H}_2\text{O}_2]_0 = 2.0 \times 10^{-5} \text{ M}$; $[\text{O}_3^-]_0 = 7.79 \times 10^{-5} \text{ M}$, $[\text{H}_2\text{O}_2]_0 = 3.50 \times 10^{-5} \text{ M}$; $[\text{O}_3^-]_0 = 9.03 \times 10^{-5} \text{ M}$, $[\text{H}_2\text{O}_2]_0 = 5.0 \times 10^{-5} \text{ M}$; $[\text{O}_3^-]_0 = 6.52 \times 10^{-5} \text{ M}$, $[\text{H}_2\text{O}_2]_0 = 7.0 \times 10^{-5} \text{ M}$; $[\text{O}_3^-]_0 = 8.07 \times 10^{-5} \text{ M}$, $[\text{H}_2\text{O}_2]_0 = 9.0 \times 10^{-5} \text{ M}$. $\text{pH} = 13.1$, $T = 25^\circ\text{C}$, $I = 0.5 \text{ M NaClO}_4$.

EVALUATION OF THE EXPERIMENTAL DATA

Some of the evaluation techniques used in ozone chemistry are based on the initial rate method and/or the steady-state approach. The main advantages of these methods are their simplicity and straightforward visualization of the results via linear plots of the reaction rate as a function of the initial concentrations. This approach can efficiently be used under specific conditions (e.g., in evaluating pulse radiolytic and other fast kinetic experiments), when only a subset of the possible reaction steps is operative. In these cases, the appropriate kinetic expressions are derived by introducing a number of simplifying assumptions. Critical evaluation of the literature data reveals that quite often oversimplified models were used, which resulted in biased results for certain rate constants even in experimentally well defined and controlled systems. Not surprisingly, the combination of the corresponding kinetic data into detailed kinetic models provided false interpretation of the overall decomposition reaction [18].

It should be noted that some of the kinetic traces are just too complex to be evaluated by classical data treatment methods. Let's consider the kinetic trace shown in Fig. 1. In this case, the initial rate method may provide some information for the very first segment of the reaction but it is useless to explain the sharp minimum at longer reaction times. This feature cannot be explained by the steady-state approach either.

Compared to the classical kinetic approach, comprehensive data treatment is based on an essentially different philosophy of handling complex reactive systems. In this case, a detailed kinetic model is postulated which includes all potential reaction steps with the corresponding initial set of rate constants obtained from the literature or estimated on the basis of the experimental data. The chemical model is represented by an ordinary differential equation system (ODE), assuming that each reaction step is elementary, and the ODE is integrated using an appropriate algorithm (e.g., the GEAR algorithm) [23]. The concentrations are calculated for each species and converted into absorbance vs. time profiles taking into account the molar absorptivities of each species at a given wavelength. The model is developed by simultaneously fitting a series of experimental kinetic curves recorded under a variety of conditions. In this process, the marginal reaction steps are eliminated from the model by sensitivity analysis. In other words, it is thoroughly tested if a given reaction step has any effect on the kinetic traces when its rate constant is systematically varied up to the diffusion-controlled limit. The data are analyzed by a nonlinear least-squares algorithm in the final stage of the evaluation [24].

The typical outcome of the comprehensive evaluation is a fairly detailed kinetic model (i.e., a set of individual reaction steps with the corresponding rate constants). Some of these parameters are obtained with relatively low uncertainties (i.e., standard deviations are similar to those obtained in classical kinetic studies), while only rough estimates or limiting values can be given for the rate constants of less significant steps. Comprehensive data treatment is often challenged on the grounds that (i) there is no perfect match between measured and calculated kinetic traces, (ii) the involvement of additional experimental data in the calculations leads to a new set of rate constants, and (iii) more than one kinetic models may provide equivalent interpretation of the same observations. Such criticism typically arises from the lack of thorough understanding of comprehensive evaluation techniques rather than from real arguments.

In a complex reaction such as ozone decomposition, there is strong kinetic coupling between various reaction steps and the applicable conditions may not be suitable to evaluate the system in sufficient detail. Thus, inferior reaction steps may alter the kinetic profiles, but their contribution to the overall process still cannot be large enough to estimate their rate constants. This introduces some uncertainty into the kinetic model and ultimately gives rise to systematic deviations between measured and calculated data. However, the noted problem by no means discredits comprehensive data treatment methods because it is associated with experimental limitations and not the evaluation procedure. Such complications remain hidden when classical evaluation techniques are used, explaining why the inconsistencies in the literature results were often overlooked before.

The need for recalibration of the kinetic model whenever new experimental data sets are included in the calculations can be understood along the same lines discussed above. In comprehensive data treatment, the pieces of kinetic information carried by the individual traces are combined as a whole and used simultaneously. Adding new traces means that more reliable information becomes available for some of the rate constants and their values can be fitted with higher confidence. This is an iterative process, that is, the model can be used to design specific experimental conditions for estimating the rate constants of otherwise insignificant reaction steps and ultimately to clarify remaining inconsistencies between measured and fitted data. The new results are incorporated into the next, amended kinetic model. Because of the cross-correlation between the fitted parameters, any change in a rate constant also affects the other values, and refitting of the expanded data sets results in somewhat different values for most of the rate constants. In other words, feeding more information into the evaluation process improves the quality of the model and the variation of the calculated rate constants is an inherent feature of the procedure.

A very important aspect of comprehensive data treatment is the validation of the kinetic model. Because of the complexity of the overall reaction, there is always a risk that the conclusions are false. This pitfall can be avoided by experimentally testing if the model correctly predicts the behavior of the system under a variety of conditions. In this respect, conditions where the system exhibits simple kinetic features are of particular interest because of the convenience of the experimental work and transparency of the results. In summary, when used with competence, comprehensive data treatment is a very powerful tool for exploring the intimate features of complex reaction systems and it outperforms classical evaluation techniques in many ways.

KINETIC MODEL FOR AQUEOUS OZONE DECOMPOSITION

The kinetic model shown in Table 1 was obtained by studying ozone decomposition as a function of pH, hydrogen peroxide, and carbonate ion concentrations. The first model was developed by studying the pH dependence of the decomposition. In subsequent stages, this model was recalibrated by including kinetic traces obtained in the presence of carbonate ion and hydrogen peroxide both separately and in combination. In the final calculations, about 60 kinetic traces recorded at 260, 430, and 600 nm were fitted simultaneously with the program package ZiTa [24]. Each trace was taken as the average of at least three replicate runs and contained at least 400 data points. The quality of fit between measured and

calculated traces is illustrated in Fig. 7. The model also predicts the concentration profiles of the ozonide ion and carbonate ion radicals reasonably well under a variety of experimental conditions [9,25]. As discussed in the following paragraphs, the results provide important insight into the details of the overall process.

Table 1 A comprehensive kinetic model for aqueous ozone decomposition.

Reaction		Rate constant ^a		References
		Fitted	Literature	
$O_3 + OH^- = HO_2^- + O_2$	k_{R1}	170 ± 2	40 – 220	[9,13,16,17,25,26]
$HO_2^- + O_3 = O_3^- + HO_2$	k_{R2}	$(3.1 \pm 0.1) \times 10^6$	5.5×10^6	[13]
$O_2^- + O_3 = O_3^- + O_2$	k_{R3}	$(7.0 \pm 0.6) \times 10^7$	1.6×10^9	[15]
$O_3^- + OH = O_2^- + HO_2$	k_{R4}	$(1.9 \pm 0.1) \times 10^{10}$	8.5×10^9	[28]
$O_3^- + OH = O_3 + OH^-$	k_{R5}	$(1.0 \pm 0.1) \times 10^{10}$	2.5×10^9	[28]
$OH + O_3 = HO_2 + O_2$	k_{R6}	$(1.0 \pm 0.1) \times 10^8$	$(0.1 - 3.0) \times 10^9$	[28,29]
$O^- + HO_2^- = O_2^- + \dot{O}H^-$	k_{R7}	$(3.2 \pm 0.4) \times 10^9$	$(0.04 - 1.0) \times 10^9$	[30,31]
$O^- + O_2^- (+ H_2O) = O_2 + 2OH^-$	k_{R8}	1.7×10^8 ^b	6.0×10^8	[32]
$O_3^- = O_2 + O^-$	k_{R9}	5.0×10^3 ^b	$(2.6 - 6.2) \times 10^3$	[33,34]
(log $K = -5.7$)	k_{-R9}	2.6×10^9 ^d	$(2.5 - 4.0) \times 10^9$	[35,36]
$HO_2 + OH^- = O_2^- (+ H_2O)$	k_{R10}	1.0×10^{10} ^c		
(log $K = 9.0$)	k_{-R10}	10 ^d		
$H_2O_2 + OH^- = HO_2^- (+ H_2O)$	k_{R11}	1.0×10^{10} ^c		
(log $K = 2.1$)	k_{-R11}	7.6×10^7 ^d		
$OH + OH^- = O^- (+ H_2O)$	k_{R12}	4.0×10^{10} ^c		
(log $K = 1.9$)	k_{-R12}	5.4×10^8 ^d		
$H^+ + OH^- = (H_2O)$	k_{R13}	1.0×10^{11} ^c		
(log $K = 13.77$)	k_{-R13}	1.7×10^{-3} ^d		
$OH + O_2^- = O_2 + OH^-$	k_{R14}	7.8×10^8 ^b	$(0.7 - 1.0) \times 10^{10}$	[37,38]
$OH + H_2O_2 = HO_2 (+H_2O)$	k_{R15}	2.7×10^7 ^b	$(1.7 - 6.5) \times 10^7$	[30]
$OH + HO_2^- = O_2^- (+H_2O)$	k_{R16}	$(8.4 \pm 0.5) \times 10^9$	$(5.6 - 8.3) \times 10^9$	[39,40]
$OH + OH = H_2O_2 (+H_2O)$	k_{R17}	e	$(5.6 - 8.3) \times 10^9$	[35,41]
$OH + HO_2 = O_2 (+H_2O)$	k_{R18}	e	$(0.7 - 1.5) \times 10^{10}$	[30,42]
$O^- + H_2O_2 = O_2^- (+H_2O)$	k_{R19}	e	5.0×10^7	[30]
$O^- + O^- (+H_2O) = HO_2^- + OH^-$	k_{R20}	e	8.0×10^9	[35]
$HCO_3^- + OH^- = CO_3^{2-} (+ H_2O)$	k_{R21}	5.0×10^9 ^c		
(log $K = 3.47$) ^d	k_{-R21}	1.7×10^6 ^d		
$CO_3^{2-} + OH = CO_3^- + OH^-$	k_{R22}	$(1.9 \pm 0.1) \times 10^8$	$(2.0 - 4.2) \times 10^8$	[20,43]
$CO_3^- + O_3^- = CO_3^{2-} + O_3$	k_{R23}	$(3.6 \pm 0.8) \times 10^7$	6.0×10^7	[44]
$CO_3^{2-} + O^- (+ H_2O) = CO_3^- + 2OH^-$	k_{R24}	$<1.0 \times 10^7$ ^b	1.0×10^7	[45]
$HCO_3^- + OH = CO_3^- (+ H_2O)$	k_{R25}	$<2.0 \times 10^7$ ^b	$(0.9 - 4.9) \times 10^7$	[39,46]
$HCO_3^- + O_2^- = CO_3^{2-} + HO_2^-$	k_{R26}	$<5.0 \times 10^4$ ^b	$(1.0 - 2.0) \times 10^6$	[30,45]
$CO_3^- + O_2^- = CO_3^{2-} + O_2$	k_{R27}	$(6.8 \pm 0.4) \times 10^9$	$(0.4 - 1.5) \times 10^9$	[45,47]
$CO_3^- + H_2O_2 = HCO_3^- + HO_2$	k_{R28}	$(2.1 \pm 0.2) \times 10^8$	8.0×10^5	[47]
$CO_3^- + HO_2^- = CO_3^{2-} + HO_2$	k_{R29}	$(3.4 \pm 0.2) \times 10^8$	6.0×10^7	[47]

^aZeroth-, first- and second-order rate constants are in M, s⁻¹ and M⁻¹ s⁻¹, respectively. Error is given for the fitted rate constant.

^bEstimated on the basis of sensitivity analysis.

^cAssuming diffusion control.

^dCalculated from the forward rate constant and the equilibrium constant.

^eNegligible under the conditions applied.

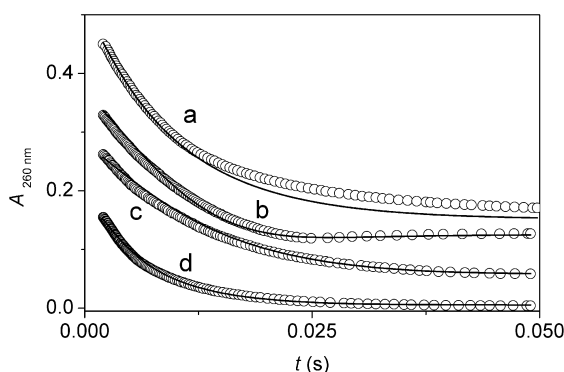


Fig. 7 Experimental (circles) and fitted (solid lines) kinetic traces. $[\text{O}_3]_0 = 1.1 \times 10^{-4} \text{ M}$, $[\text{H}_2\text{O}_2]_0 = 2.0 \times 10^{-6} \text{ M}$, $\text{pH} = 12.2$, trace is shifted by + 0.15 AU, time scale is divided by 4 (a); $[\text{O}_3]_0 = 8.5 \times 10^{-5} \text{ M}$, $[\text{H}_2\text{O}_2]_0 = 2.0 \times 10^{-6} \text{ M}$, $\text{pH} = 13.1$, trace is shifted by + 0.10 AU (b); $[\text{O}_3]_0 = 7.3 \times 10^{-5} \text{ M}$, $[\text{H}_2\text{O}_2]_0 = 8.0 \times 10^{-6} \text{ M}$, $\text{pH} = 12.7$, trace is shifted by + 0.05 AU (c); $[\text{O}_3]_0 = 5.6 \times 10^{-5} \text{ M}$, $[\text{H}_2\text{O}_2]_0 = 5 \times 10^{-5} \text{ M}$, $\text{pH} = 11.0$ (d); $T = 25 \text{ }^\circ\text{C}$, $I = 0.5 \text{ M NaClO}_4$.

The initiation sequence

There is an intense debate about the rate constant of the initiation step (R1) in the literature. Reported values are in the range of $40\text{--}220 \text{ M}^{-1} \text{ s}^{-1}$ [9,13,16,17,25,26]. Although there is mounting evidence that this rate constant was underestimated in early studies and in reality it needs to be somewhere around $180 \text{ M}^{-1} \text{ s}^{-1}$, the most frequently used value is still $70 \text{ M}^{-1} \text{ s}^{-1}$. The highest rate constant for this step was reported by Elovitz and von Gunten on the basis of kinetic modeling of ozone decomposition [26]. Oddly enough, these authors discard their own results in spite of the fact that they obtained a much better fit using $220 \text{ M}^{-1} \text{ s}^{-1}$ instead of $70 \text{ M}^{-1} \text{ s}^{-1}$, and experimental data for the oxidation of *p*-chlorobenzoic acid corroborated their finding. They conclude that the latter value must be correct because it was measured in a “carefully defined and controlled system”. Their argument is acceptable in that there is no reason to challenge the reliability of earlier experiments. However, simplified models in those studies yielded grossly underestimated rate constants for the initiation step. An inspection of the model in Table 1 reveals that O_3 is not only consumed but also regenerated in step R5. Consequently, the experimentally observed rate of ozone decay is considerably smaller than the rate of R1 and any model that omits the feedback path predicts only an apparent value for k_{R1} .

Early model calculations already indicated the discrepancies with the initiation rate constant and suggested considerably higher value than $70 \text{ M}^{-1} \text{ s}^{-1}$ [18]. On the basis of pH-dependent experiments, our first estimate for k_{R1} ($140 \text{ M}^{-1} \text{ s}^{-1}$) was somewhat biased because the values for k_{R2} and k_{R3} could not be determined and the kinetic role of these steps was overestimated on the basis of literature data [9]. Detailed studies on hydrogen peroxide catalysis cured the problem because systematic variation of the H_2O_2 concentration made it possible to resolve each rate constant separately in the initiation sequence and estimate their rate constants with reasonable precision. The new result, $k_{\text{R1}} = 170 \text{ M}^{-1} \text{ s}^{-1}$, is in excellent agreement with a recent literature value [17] and also supported by the results obtained for carbonate ion inhibition (vide infra).

Chain carriers

Chain carrier radicals are of primary importance in aqueous ozone decomposition. It is a generally accepted concept that the dominant propagation steps include the OH radical. However, calculations on the basis of the kinetic model suggest a mechanistic changeover as a function of pH. In very alkaline solution, the initiation sequence is relatively fast and consequently the chain is short. Under such con-

ditions, the accumulation of the O_3^- radical is observed and the overall process is controlled by the reactions of this species. The system gradually switches to the OH channels when the pH is decreased (i.e., when the initiation step becomes slower). This pattern changes considerably in the presence of H_2O_2 . Hydrogen peroxide catalyzes the decomposition (R2), enhances the OH formation (R9, R12), and its direct reaction with OH accelerates the reaction path via the superoxide radical (R15, R16).

Because of the extreme reactivity of the OH radical, only specific kinetic methods are suitable to obtain direct kinetic information for its reactions. The results presented in Table 1 clearly demonstrate that careful design of the experiments combined with comprehensive data treatment makes it possible to subtract reliable kinetic information for this species from classical stopped-flow measurements. The rate constants for the dominant reaction steps of the OH radical (R4, R5, R16) could be estimated with reasonable certainty, and it was also confirmed that a few other reactions of OH and O^- (R7, R8, R14, R15) have a limited role in the overall process. Four other reactions of these species (R17–R20) were excluded from the kinetic model on the basis of sensitivity analysis.

In a few papers, the reactions of the HO_3 radical were also postulated in ozone decomposition models [13–15]. As discussed in earlier reports in detail, there are fundamental problems with the literature values for the pK_a and the decomposition rate constant of this species [9,27]. Nevertheless, we made several attempts to include the HO_3 radical in our model calculations. The results strongly suggest that the reactions of this species can be excluded from the kinetic model. The same applies to the HO_4 radical, which was considered to be a reservoir species in this reaction by Staehelin and coworkers [13,14].

Carbonate ion inhibition, validation of the kinetic model

There is a consensus that the inhibitory effect of carbonate ion on ozone decomposition is due to its ability to scavenge the OH radical (R22). However, model calculations confirmed that this reaction alone cannot explain the experimental observations. Most importantly, the kinetic model needs to include reaction steps, which prevent the accumulation of the carbonate ion radical and also explain the reduced formation of the O_3^- radical at high pH. In this respect, it should be noted that CO_3^- appears as an intermediate at very low concentration level and can be detected only at relatively high pH and in very narrow concentration ranges of the reactants. It was confirmed that the dominant channel for the removal of CO_3^- is its reaction with O_3^- (R23) [25]. This reaction has a combined retarding effect on ozone decay. It removes an important chain carrier and at the same time regenerates ozone. It follows that the inhibition has a very dynamic feature because the initiation rate is not affected at all by carbonate ion and the phenomenon needs to be interpreted in terms of relatively fast recycling of ozone.

Apart from the two dominant steps, other reactions also affect the overall kinetics. Once again, the model needed to be recalibrated when kinetic traces recorded in the presence of carbonate ion and hydrogen peroxide were included in the fitting procedure. This can be understood by considering that the addition of H_2O_2 increased directly or indirectly the relative kinetic weight of several reaction steps (R27–R29).

The kinetic model predicts that the decomposition occurs in a simple pseudo-first-order process when carbonate ion is present at relatively high concentration levels. Under such conditions, the rate-determining step is R1, and the reaction sequence leading to the formation of the OH radical (R2, R9), the corresponding protonation steps, quenching of OH (R22) as well as regeneration of ozone (R23) are very fast. By introducing the steady-state approach for the chain carrier, the following expression can be derived for k_{obs} :

$$k_{obs} = 1.5 k_{R1} [OH^-] \quad (4)$$

Experimental observations at 260 nm confirmed pseudo-first-order behavior and the validity of the above expression with $k_{R1} = 173 \text{ M}^{-1} \text{ s}^{-1}$ [25]. The excellent agreement with the rate constant shown in Table 1 lends strong support to the validity of the proposed kinetic model.

CONCLUDING REMARKS

In spite of tremendous advancement in our understanding of aqueous ozone decomposition in recent years, there are a number of critical problems still to be solved. Most importantly, further work needs to be done to test the validity of the model under neutral and alkaline conditions. It is anticipated that the initiation step(s) may differ significantly by changing the conditions, but some of the main propagation steps are expected to be operative in the entire pH range. Thus, one of the main tasks is to carefully test the implications of the results surveyed here in a broader context. Another aspect is to expand the model to practical applications, most specifically to AOPs in both batch and continuous systems. This presents new exciting challenges from both experimental and computational points of view. Recent technical developments in experimental techniques, as well as the spread of new evaluation methods, will certainly be instrumental in addressing such problems and opening new perspectives in this field.

ACKNOWLEDGMENT

The Hungarian Research fund is acknowledged for financial support under grant No. OTKA T042755.

REFERENCES

1. <<http://nobelprize.org/chemistry/laureates/1995/index.html>> (1995).
2. S. D. Razumovski, G. E. Zaikov. *Ozone and its Reactions with Organic Compounds*, Elsevier, New York (1984).
3. G. C. White. *Handbook of Chlorination and Alternative Disinfectants*, Van Nostrand Reinhold, New York (1992).
4. J. Hoigné. In *The Handbook of Environmental Chemistry*, Vol. 5, Part C, J. Hrubec (Ed.), p. 84, Springer Verlag, Berlin (1998).
5. U. von Gunten. *Water Res.* **37**, 1443 (2003).
6. U. von Gunten. *Water Res.* **37**, 1469 (2003).
7. K. Ikehata, M. Gamal El-Din. *Ozone Sci. Eng.* **26**, 327 (2004).
8. A. Nemes, I. Fábíán, G. Gordon. *Ozone Sci. Eng.* **22**, 287 (2000).
9. A. Nemes, I. Fábíán, G. Gordon. *Inorg. React. Mech.* **2**, 327 (2000).
10. H. Taube, W. C. Bray. *J. Am. Chem. Soc.* **62**, 3357 (1940).
11. T. M. Lesko, A. J. Colussi, M. R. Hoffmann. *J. Am. Chem. Soc.* **126**, 4432 (2004).
12. L. Forni, D. Bahnemann, E. J. Hart. *J. Phys. Chem.* **86**, 255 (1982).
13. J. Staehelin, J. Hoigné. *Environ. Sci. Technol.* **16**, 676 (1982).
14. J. Staehelin, R. E. Bühler, J. Hoigné. *J. Phys. Chem.* **88**, 5999 (1984).
15. (a) R. E. Bühler, J. Staehelin, J. Hoigné. *J. Phys. Chem.* **88**, 2560 (1984); (b) erratum: R. E. Bühler, J. Staehelin, J. Hoigné. *J. Phys. Chem.* **88**, 5450 (1984).
16. H. Tomiyasu, H. Fukutomi, G. Gordon. *Inorg. Chem.* **24**, 2962 (1985).
17. B. K. Bezboura, D. A. Reckhow. *Ozone Sci. Eng.* **26**, 345 (2004).
18. K. Chelkowska, D. Grasso, I. Fábíán, G. Gordon. *Ozone Sci. Eng.* **14**, 33 (1992).
19. G. Czapski, L. M. Dorfman. *J. Phys. Chem.* **68**, 1169 (1964).
20. J. L. Weeks, J. Rabani. *J. Phys. Chem.* **70**, 2100 (1966).
21. K. Sehested, H. Corfitzen, J. Holcman, E. J. Hart. *J. Phys. Chem. A* **102**, 2667 (1998).
22. Z. Szíjgyártó. Thesis, University of Debrecen (2001).

23. A. C. Hindmarsh. GEAR: Ordinary Differential Equation Solver, Rev. 2, Lawrence Livermore Laboratory, Livermore, CA (1972).
24. G. Peintler. ZITA 5.0: A Comprehensive Program Package for Fitting Parameters of Chemical Reaction Mechanisms, Szeged (1999).
25. A. Nemes, I. Fábián, R. van Eldik. *J. Phys. Chem. A* **104**, 7995 (2000).
26. M. S. Elovitz, U. von Gunten. *Ozone Sci. Eng.* **21**, 239 (1999).
27. L. E. Bennett, P. Warlop. *Inorg. Chem.* **29**, 1975 (1990).
28. K. Sehested, J. Holcman, E. Bjergbakke, E. J. Hart. *J. Phys. Chem.* **88**, 4144 (1984).
29. D. Bahnemann, E. J. Hart. *J. Phys. Chem.* **86**, 252 (1982).
30. Farhataziz, A. B. Ross. *Natl. Stand. Ref. Data Ser., Natl. Bur. Stand.* **59**, 113 (1977).
31. H. Christensen, K. Sehested, H. Corfitzen. *J. Phys. Chem.* **86**, 1588 (1982).
32. K. Sehested, J. Holcman, E. Bjergbakke, E. J. Hart. *J. Phys. Chem.* **86**, 2066 (1982).
33. J. A. Elliot, D. R. McCracken. *Radiat. Phys. Chem.* **33**, 69 (1989).
34. K. Bobrowski, J. P. Suwalski, Z. P. Zagorski. *Int. J. Radiat. Phys. Chem.* **8**, 527 (1976).
35. J. Rabani, M. S. Matheson. *J. Phys. Chem.* **70**, 761 (1966).
36. G. E. Adams, J. W. Boag, B. D. Michael. *Proc. R. Soc. London, Ser. A* **289**, 321 (1966).
37. G. Beck. *Int. J. Radiat. Phys. Chem.* **1**, 361 (1969).
38. J. Rabani, S. O. Nielsen. *J. Phys. Chem.* **73**, 3736 (1969).
39. G. V. Buxton. *J. Chem. Soc., Faraday Trans.* **68**, 2150 (1969).
40. J. Rabani. *Adv. Chem. Ser.* **81**, 131 (1968).
41. A. J. Elliot. *Radiat. Phys. Chem.* **34**, 753 (1989).
42. K. Sehested, O. L. Rasmussen. *J. Phys. Chem.* **72**, 626 (1968).
43. P. K. A. Hong, M. E. Zappi, C. H. Kuo, D. Hill. *J. Environ. Eng.* **122**, 58 (1996).
44. G. V. Buxton, C. L. Greenstock, W. P. Helman, A. B. Ross. *J. Phys. Chem. Ref. Data* **17**, 513 (1988).
45. A. B. Ross, P. Neta. *Natl. Stand. Ref. Data Ser., Natl. Bur. Stand.* **65**, 62 (1979).
46. G. V. Buxton, N. D. Wood, S. Dyster. *J. Chem. Soc., Faraday Trans. 1* **84**, 1113 (1988).
47. D. Behar, G. Czapski, I. Duchovny. *J. Phys. Chem.* **74**, 2206 (1970).